New Tris(hydroxypyridinones) as Iron and Aluminium Sequestering Agents: Synthesis, Complexation and In Vivo Studies

Sílvia Chaves,[a] Sérgio M. Marques,[a] André M. F. Matos,[a] Andreia Nunes,[a] Lurdes Gano,[b] Tiziano Tuccinardi,[c] Adriano Martinelli,[c] and M. Amélia Santos*[a]

Abstract: Two new tripodal tris(3-hydroxy-4-pyridinone) hexadentate chelators—NTA(BuHP)$_3$ and NTP(PrHP)$_3$ (NTA = nitrilotriacetic acid, NTP = nitrilotripropionic acid, HP = hydroxypyridone)—have been developed and studied in solution for their iron and aluminium binding affinity, and also assayed in vivo for their capacity to remove metal from an animal model that is overloaded. These chelators are positional isomers, possessing identical general structures based on aminotricarboxylic acid skeletons attached to three bidentate 3-hydroxy-4-pyridinones (3,4-HPs), but differing in the position of the amide linkage along the chelating "arm". In spite of expected differences in the tripodal ligands, such as acidity and hydrogen-bonding networks, they share important properties, namely, a mild hydrophilic character ($\log P$ ca. -1.2 to -1.4) and a strong chelating affinity for Fe and Al (pFe = 27.9 and pAl = 22.0 for NTA(BuHP)$_3$; pFe = 29.4 and pAl = 22.4 for NTP-(PrHP)$_3$). They also evidenced identical effects on the biodistribution and on the excretion of a radiotracer (^{67}Ga) previously administered to mice, as models of iron overload animals. Comparison of the new compounds with reported analogues shows good improvement in terms of solution and in vivo sequestering properties, thus giving support to expectations about their potential clinical application as metal removal agents.

Keywords: biodistribution · chelates · hydroxypyridinones · iron · sequestering agents

Introduction

Iron is an essential bioelement, but when in excess it is toxic. Iron overload diseases, such as hemochromatosis or beta-thalassemia-associated transfusion hemosiderosis, can be fatal unless patients follow iron-chelating therapy protocols.[1] Environmental exposure or therapeutic contamination can also lead to accumulation of other hard metal ions (e.g., aluminium) in certain organs, resulting in serious diseases in the brain (dialysis encephalopathy) or in the bone (osteomalacia).[2,3] To prevent or relieve these problems, the design of new orally active specific chelators has been a major objective and a number of synthetic chelators have been reported.[4,5]

Desferrioxamine B (DFO) was the first and the only hexadentate ligand approved by the Food and Drug Administration (FDA) for chelating therapy of patients with transfusion iron overload. However, the drawbacks associated with this therapeutic, such as the low patient compliance due to the need for daily subcutaneous (sc) or intravenous (iv) administration, led to the investigation of new chelators.[4]

Major advances in terms of new iron chelators appeared in form of the 3-hydroxy-4-pyridinone (3,4-HP) family of compounds, that is, after the disclosure of Deferiprone (DFP, 1,2-dimethyl-3-hydroxypyridin-4-one) as an orally active drug for the treatment of iron overload.[6] This type of compound has a high affinity for hard metal ions and favourable toxicity profiles; on the other hand, they can be easily designed for extra-functionalisation to guarantee high bioavailability as well as targeting properties. Therefore, this family of bidentate chelators has long been considered good

[a] Prof. Dr. S. Chaves, Dr. S. M. Marques, Dipl.-Chem. A. M. F. Matos, Dipl.-Chem. A. Nunes, Prof. Dr. M. A. Santos
Centro de Química Estrutural, Instituto Superior Técnico
Av. Rovisco Pais 1, 1049-001 Lisboa (Portugal)
Fax: (+351) 21-8464455
E-mail: masantos@ist.utl.pt

[b] Dr. L. Gano
Instituto Tecnológico e Nuclear, Estrada Nacional N° 10
2686-953 Sacavém (Portugal)

[c] Dr. T. Tuccinardi, Prof. Dr. A. Martinelli
Università degli Studi di Pisa
Dipartimento di Scienze Farmaceutiche
Via Bonanno 6, 56126 Pisa (Italy)

pharmaceutical targets for chelating therapeutics[7–9] or even metallodrugs.[10] Nevertheless, some drawbacks (toxicity) associated with the low denticity of DFP and concomitant high dosage demands for competition with bioligands led to the search for ligands with increased denticity. Aside from the recent emergence of new tridentate iron chelators approved by the FDA (desferasirox or ICL670),[11] several research groups have been implementing drug design strategies to increase the ligand denticity. Specifically, some polydentate 3,4-HP-based chelators have been developed, that is, tetradentate ligands, to be used alone or in combined-ligand therapeutic protocols,[12,13] and hexadentate ligands, to fulfil the metal coordination by the formation of 1:1 M^{3+}–L (metal–ligand) complexes with improved thermodynamic and kinetic stability.[14,15]
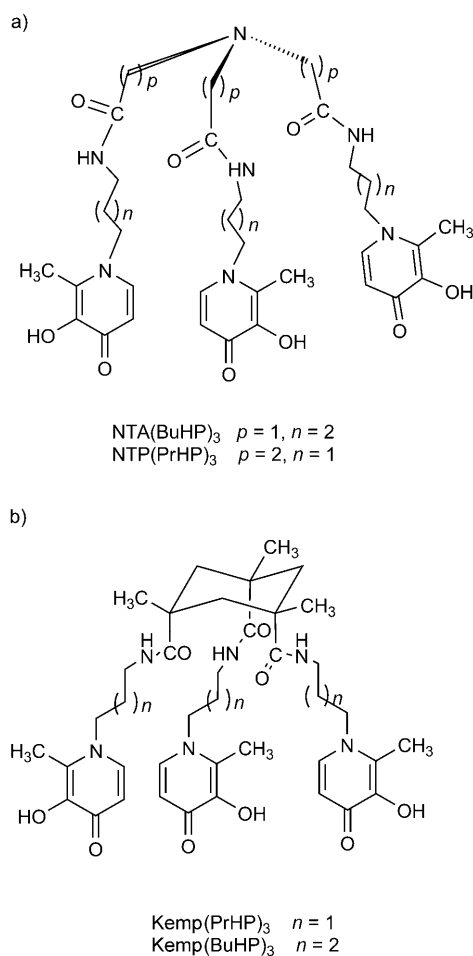
Herein, we report results on the development and study of two new hydroxypyridinone-based tripodal hexadentate chelators with three 3,4-HP units appended to amino-tris-carboxylic anchoring skeletons, namely, nitrilotriacetic acid (NTA) and nitrilotripropionic acid (NTP) (Scheme 1a). Besides the design and the synthetic strategy of the new com-

pounds, this paper is focused on the study of the physico-chemical properties of ligands and complexes in solution, especially those related to the lipo-hydrophilic character and complexation ability towards iron(III) and aluminium(III), as well as some modelling studies on the iron complex structures. Their in vivo behaviour as potential sequestering agents is also assessed, that is, their ability for the ^{67}Ga mobilisation from mice previously injected with this radiotracer, as an animal model of Fe or Al overload.

Results and Discussion

Design and chemistry of the compounds: Notwithstanding the high interest in 3,4-HPs as iron chelating agents and the importance of polydenticity as a determining factor for the thermodynamic stability of the metal complexes, up to around five years ago only bidentate 3,4-HP compounds had been explored, as opposed to the other HP classes.[15] Therefore, we have implemented a strategy for developing polydentate 3,4-HP-based compounds by attachment of two or three N-alkylamine-3,4-HP ("arms") to suitable polycarboxylate-containing skeletons to form, respectively, tetra- and hexadentate ligands pre-organised to wrap and coordinate the metal ions.[16] For the hexadentate ligands, tris(3,4-HP), we first appended three of the chelating arms to a Kemp acid, a cyclohexane-based scaffold containing three carboxylic groups in axial positions (Scheme 1b).[15] Despite the high stability of the corresponding M^{3+} complexes, the fully coordinated species were quite insoluble in water. Therefore, to bring some hydrophilicity to the chelator/complex system, we designed a new set of compounds based on aminotricarboxylic acid skeletons with a central amine group as the anchoring point for the three carboxylic acids. Based on a preliminary modelling study, it seemed that, between the apical tertiary amine and the 3,4-HP chelating units, a spacer containing five methylenic groups plus an amide bond (for the linkage between the anchoring carboxylic and the amine groups of the HP arms) was well suited for wrapping the iron. Accordingly, two tris(3,4-HP) chelators were developed with arms of the type $-(CH_2)_p-C(O)NH-(CH_2)_m$, in which $p+m=5$, but with different peptide bond positions: $p=1$, $m=4$ for NTA(BuHP)$_3$; $p=2$, $m=3$ for NTP-(PrHP)$_3$.

The synthetic route for the preparation of the compounds involved the coupling of the aminotriacid skeletons (NTA and NTP) with the free amine group of an N-alkylamine, O-benzylated monohydroxypyridinone arm (alkyl=butyl or propyl), through activation of the anchoring carboxylic groups with O-(benzotriazol-1-yl)-N,N,N′,N′-tetramethyluronium tetrafluoroborate (TBTU), in dry DMF at low temperature and under nitrogen. This methodology afforded the corresponding benzyl-protected tris-3,4-HP derivatives, which were isolated by recrystallisation or silica-gel chromatography. The final products were obtained by removal of the protecting groups through standard methods of hydrogenolysis.

a)

NTA(BuHP)$_3$ $p = 1$, $n = 2$
NTP(PrHP)$_3$ $p = 2$, $n = 1$

b)

Kemp(PrHP)$_3$ $n = 1$
Kemp(BuHP)$_3$ $n = 2$

Scheme 1. Structural formulae of the studied (a) and reported (b) hexadentate 3,4-HP ligands.

Physico-chemical characterisation of the compounds: The new tripodal tris(hydroxypyridinones) ($NTA(BuHP)_3$ and $NTP(PrHP)_3$) were studied in terms of their acid–base properties and lipo-hydrophilic character. Both compounds were isolated in the neutral form (H_3L), but when fully protonated (H_7L^{4+}) they have seven dissociable protons. The protonation processes were mainly studied by potentiometry and fitting analysis of the corresponding titration data, but, in the case of $NTA(BuHP)_3$, a ^1H NMR spectroscopic titration was also performed to identify the respective protonation sequence and to determine the very low $\log K_7$ value (< 2). Table 1 summarises the stepwise protonation constants ($\log K_i$), calculated for the compounds under study, as well as reported values for the tris(hydroxypyridinone)–Kemp acid derivatives ($Kemp(PrHP)_3$ and $Kemp(BuHP)_3$)[15] and for the commercial drug DFP.[17]
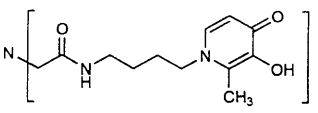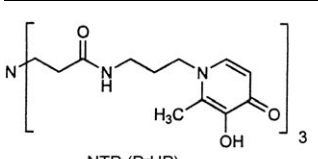
The potentiometric studies revealed that $NTA(BuHP)_3$ and $NTP(PrHP)_3$ have three protonation constants with values in the range of 8.9–10, attributable to the hydroxyl groups of the three hydroxypyridinone moieties, as well as three other protonation constants with values around 2.3–3.9 attributed to the protonation of the pyridinyl nitrogen atoms of the same moieties (see Table 1). The calculated protonation constants for these two processes are analogous to the corresponding values found in the literature (9.2–10.2/2.9–4[15] and 9.77/3.62[17]) for the Kemp derivatives and DFP, respectively. Moreover, the titration curve of $NTP(PrHP)_3$ shows a further intermediate buffer zone at around pH 7, which is attributed to the protonation of the backbone amine group. Its $\log K$ value (6.77) is much lower than that for NTP ($\log K_1 = 9.65$),[20] which can be ascribed to intramolecular hydrogen bonds of the type CONH···N, in a probable trifurcated geometry with the apical tertiary amine of the NTP skeleton. In the case of $NTA(BuHP)_3$, the $\log K$ value corresponding to the protonation of the apical amine appeared to be quite low when calculated by potentiometry and so a ^1H NMR spectroscopic titration was carried out (see Figure 1). Analysis of ^1H NMR titration curve profiles suggests that the $NTA(BuHP)_3$ protonation sequence follows the order: hydroxyl groups (at pD ≈ 11, peaks 1 and 2 are downfield shifted), pyridinyl nitrogen atoms (downfield shifts of peaks 1–3 and 6–8 at pD ≈ 4.5); apical N-amine group (downfield shift of peak 4 for pD < 3). This lowest pD buffer region indicates an enormous decrease in the protonation constant of the apical nitrogen compared with the corresponding parent compound, NTA ($\log K_1 = 9.2$).[20] This unexpectedly low value obtained for the protonation of this apical amine group can be explained by the formation of intramolecular hydrogen-bonding (CONH···N) networks that are stronger for $NTA(BuHP)_3$ ($p = 1$) than for $NTP(PrHP)_3$ ($p = 2$), due to the formation of five- and six-membered ring intermediates, respectively (see Scheme 1).

Despite the acidity differences in the backbone ammonium proton, the remaining protonation constants for both ligands are very similar because the corresponding basic centres are quite far away from the anchoring skeleton and only very negligible differences in the electron-donation effect could result from the homologous alkylic spacers.

Table 1. Stepwise protonation constants ($\log K_i$) and partition coefficients ($\log P$) for a set of tripodal compounds and DFP, as well as the global formation constants of their M^{3+} complexes ($T = (25.0 \pm 0.1)$°C, $I = 0.1$ M KCl).

Ligand	$\log K_i$	$M_pH_qL_r$ (p,q,r)	$\log \beta$ ($Fe_pH_qL_r$)	$\log \beta$ ($Al_pH_qL_r$)	$\log P$
$NTA(BuHP)_3$	9.98(2)	(1,5,1)	42.30(2)[a]	–	
	9.83(3)	(1,4,1)	40.81(5)[a]	37.45(4)	
	8.94(4)	(1,2,1)	38.53(3)[a]	33.55(1)	
	3.88(4)	(1,0,1)	33.50(1)[a]	27.65(6)	−1.40
	3.11(5)				
	2.35(5)				
	1.4(1)[b]				
		$pM^{[c]}$	27.9[d]	22.0	
$NTP(PrHP)_3$	9.946(9)	(1,5,1)	47.62(5)	44.69(6)	
	9.84(1)	(1,3,1)	45.29(5)	40.01(5)	
	9.091(8)	(1,1,1)	40.56(3)	34.72(4)	
	6.77(1)	(1,0,1)	35.21(1)	28.13(3)	−1.24
	3.81(1)				
	3.14(1)				
	2.76(2)				
		$pM^{[c]}$	29.4	22.4	
$Kemp(PrHP)_3$[15]	10.07(4)	(1,4,1)	41.50(2)	39.33(2)	
	9.89(4)	(1,2,1)	38.91(2)	33.62(3)	
	9.18(5)	(1,0,1)	33.98(3)[e]	27.21(1)	−1.04
	3.98(3)				
	3.25(3)				
	2.91(4)				
		$pM^{[c]}$	28.0	21.2	
$Kemp(BuHP)_3$[15]	10.15(3)	(1,4,1)	41.98(2)	39.84(3)	
	9.91(3)	(1,2,1)	39.08(3)	33.87(1)	
	9.21(4)	(1,0,1)	32.97(6)[e]	27.95(1)	−0.62
	4.05(4)				
	3.38(3)				
	3.10(3)				
		$pM^{[c]}$	26.8	21.8	
DFP[17]	9.77	(1,0,1)	15.14	12.20	
	3.62	(1,0,2)	26.68	23.25	−0.85
		(1,0,3)	35.92	32.62	−1.03[18]
		$pM^{[c]}$	19.3[19]	16.0[19]	

[a] Values determined in 3% DMSO. [b] Value determined by ^1H NMR titration. [c] pM values at pH 7.4 ($C_M = 10^{-6}$ M, $C_L/C_M = 10$). [d] No precipitation in the concentration conditions of pM determination. [e] Determined spectrophotometrically by competition with ethylenediaminetetraacetic acid (EDTA).
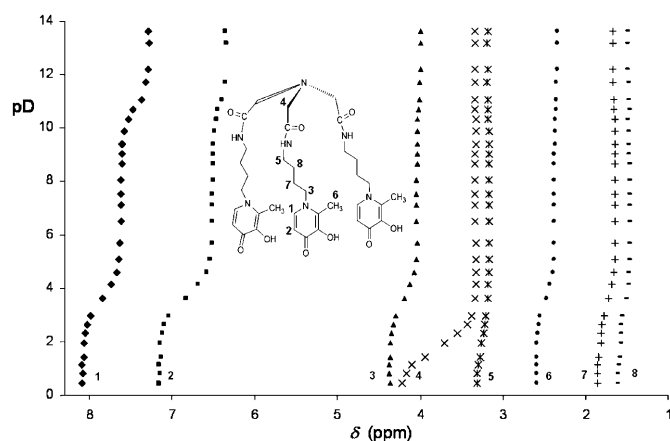
Figure 1. ^{1}H NMR spectroscopy titration curves of NTA(BuHP)$_3$ ($C_L = 7.3 \times 10^{-4}$ M).

At physiological pH, the predominant form for both compounds is the neutral species H$_3$L (ca. 82 % for NTP(PrHP)$_3$ and 98 % for NTA(BuHP)$_3$). Thus, some lipophilic nature can be expected for both ligands, although the lipo-hydrophilic character is not only determined by the molecular charge, but also by the capacity to establish solute–solvent interactions. The lipophilicity of these compounds was assessed through the calculation of their partition coefficients (log P) between 1-octanol and a Tris-buffered aqueous phase at pH 7.4. Analysis of the results given in Table 1 shows that NTA(BuHP)$_3$ and NTP(PrHP)$_3$ present similar log P values, but due to the hydrophilic character of the anchoring groups these compounds are more hydrophilic than the Kemp derivatives and DFP. Although for both the compounds the molecular weight exceeded the value suggested by the Lipinski rule for oral bioavailability (500 Da);[21] tissue and cell permeability can also be favoured by other descriptors.

Solution metal-complexation studies: The chelating ability of the compounds towards iron(III) and aluminium(III) was estimated on the basis of the global formation constants of their complexes, which were determined by UV/Vis spectrophotometric (PSEQUAD program)[22] and potentiometric (HYPERQUAD program)[23] techniques. Iron complexation was studied by spectrophotometry due to the high iron-chelating affinity of both compounds and concomitant complete formation of the complexes at the beginning of the potentiometric titration. To overcome the low water solubility of the neutral FeL complex with NTA(BuHP)$_3$, the predominant species above around pH 2.5, the iron complexation was studied in a 3 % (v/v) DMSO/water medium. Even so, it was impossible to pursue the titration over pH ≈ 5.5 since precipitation occurred, probably due to the formation of the neutral complex and/or mixed hydroxo-ligand complexes under these experimental conditions. For pH < 2, both systems were also studied spectrophotometrically by using a batch titration in which the amount of acid to be added was calculated for the total volume of solution used. The stability

constants calculated herein for the M^{3+} complexes are presented in Table 1, together with values previously determined for the Kemp derivatives[15] and DFP.[17–19]

Data analysis of the electronic spectra obtained for the Fe^{3+}–NTA(BuHP)$_3$ system (see Figure 2, top) indicates the existence of four complexes, presumably FeH$_5$L, FeH$_4$L,
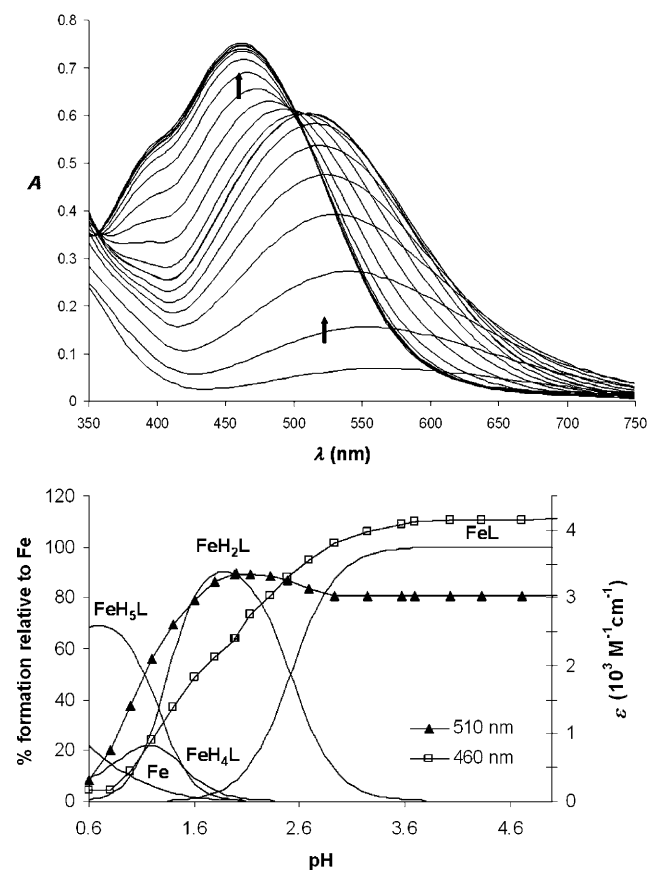

Figure 2. Top) Electronic spectra for the 1:1 Fe^{3+}–NTA(BuHP)$_3$ system, pH 0.6–5.0. Bottom) Species distribution curves for the same system with molar extinction coefficients at the maximum absorption wavelengths ($C_L/C_{Fe} = 1$, $C_L = 1.8 \times 10^{-4}$ M).

FeH$_2$L or FeL, which have one, two or three hydroxypyridinone chelating moieties, respectively, coordinated to Fe^{III}. This model is supported by analysis of the data shown in Figure 2, bottom, containing the species distribution curves for the proposed equilibrium model merged with some experimental spectral data, that is, the absorptivity at two characteristic wavelengths (510 and 460 nm). The maximum absorption at 510 nm ($\varepsilon = 3353$ M^{-1}cm^{-1}) corresponds to the charge-transfer band of the tetra-coordinated (bischelate) complex (FeH$_2$L^{2+}), whereas that at 460 nm ($\varepsilon = 4153$ M^{-1}cm^{-1}) corresponds to the hexa-coordinated (trischelate) complex (FeL). These spectral parameters are according to literature data for Fe^{3+}–(3-hydroxy-4-pyridinone) complexes.[24] The refined model also includes two bis-coordinated complexes, FeH$_4$L^{4+} and FeH$_5$L^{5+}, appearing at pH < 2, with a maximum absorption at around 560 nm, the

last complex species with the apical backbone nitrogen protonated.

Regarding the Fe^{3+}–$NTP(PrHP)_3$ system, the spectrophotometric titration curves (Figure 3, top) also show two absorption maxima at 510 ($\varepsilon = 3490\,M^{-1}cm^{-1}$) and 460 nm ($\varepsilon = 4750\,M^{-1}cm^{-1}$), which, according to our model, should correspond to the tetra- (FeH_3L) and hexa-coordinated complex species ($FeHL$ or FeL), respectively (see Figure 3, bottom). Below pH 2, both the bis-coordinated (FeH_5L) and the tetra-coordinated (FeH_3L) species are present.
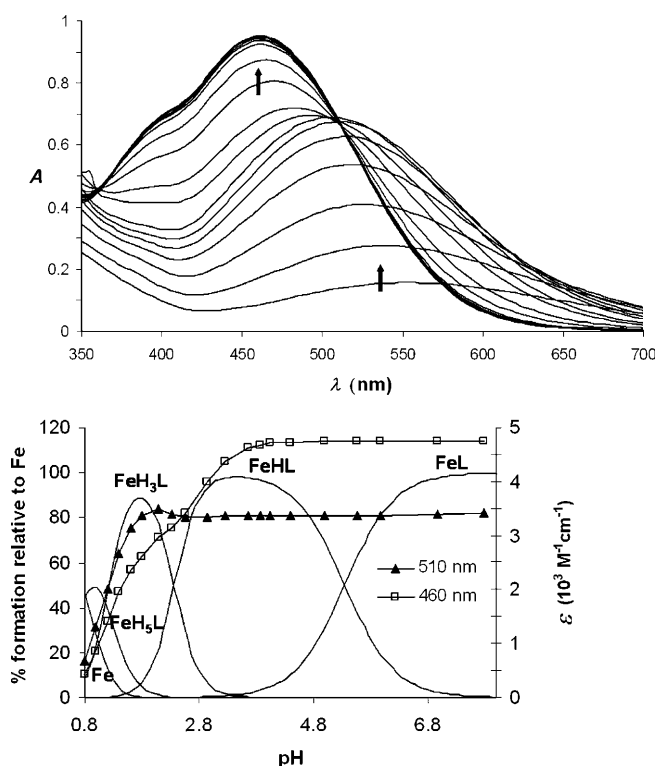

Figure 3. Top) Electronic spectra for the 1:1 Fe^{3+}–$NTP(PrHP)_3$ system, pH 0.8–8.0. Bottom) Species distribution curves for the same system with molar extinction coefficients at the maximum absorption wavelengths ($C_L/C_{Fe} = 1$, $C_{Fe} = 1.6 \times 10^{-4}\,M$).

ESI-MS measurements, performed for solutions of the Fe^{3+}–$NTA(BuHP)_3$ and Fe^{3+}–$NTP(PrHP)_3$ systems under (1:1) stoichiometric conditions at pH 3.21 and 3.66, respectively, confirmed the existence of the iron complexes as the species $[Fe(L-H)]^{2+}$ (390.3) and $[Fe(L-2H)]^+$ (779.6) for both systems.

In summary, both ligands present a similar iron complexation behaviour, although considerable differences are associated with the protonation of the apical nitrogen atom in the ligand backbone structure, namely, the unexpectedly low $\log K_7$ value found for $NTA(BuHP)_3$ (1.4) relative to NTP-$(PrHP)_3$ (6.77). Thus, for the Fe^{3+}–$NTA(BuHP)_3$ system, the monochelated species FeH_5L appears only at very low pH values, whereas the last deprotonation of the Fe^{3+}–NTP-$(PrHP)_3$ system occurs at higher pH values and so $FeHL$ is

the major hexa-coordinated complex (tris-chelated species). Also, some solubility problems, due to the presence of the neutral FeL complex, are less critical for the Fe^{3+}–NTP-$(PrHP)_3$ system because in this case that species is only predominant at pH values higher than about 5.5.

The study of Al^{3+} complexation in solution was performed by potentiometry under 1:1 stoichiometric conditions. Figure 4 shows the species distribution curves for both
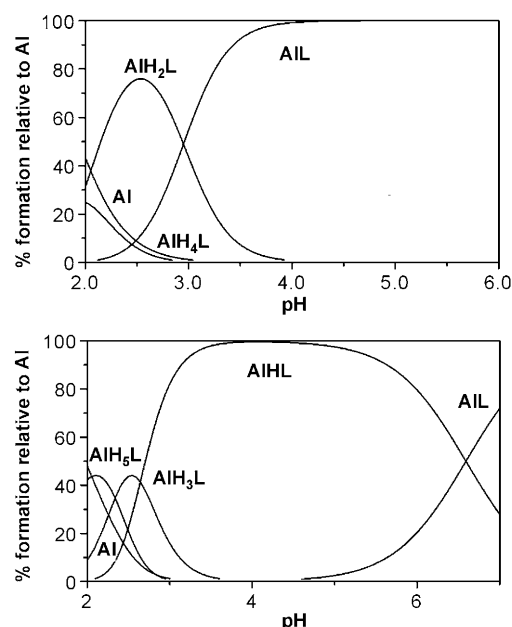

Figure 4. Species distribution curves for the 1:1 Al^{3+}–L systems with $NTA(BuHP)_3$ (top) and $NTP(PrHP)_3$ (bottom) ($C_{Al}/C_L = 1$, $C_L = 1.0 \times 10^{-3}\,M$).

Al^{3+}–ligand systems, evidencing the predominance of the hexa-coordinated tris-chelated species even in acidic conditions (pH > 3). ESI-MS spectra of 1:1 solutions for the Al^{3+}–$NTA(BuHP)_3$ (pH 3.89) and Al^{3+}–$NTP(PrHP)_3$ (pH 4.00) systems confirmed the presence of the complex species $[Al(L-H)]^{2+}$ (375.9) and $[Al(L-2H)]^+$ (750.6).

Analysis of the data reported in Table 1, namely, the pM values at physiological pH, indicates that the chelating abilities of both compounds towards aluminium are quite similar, whereas $NTP(PrHP)_3$ seems to be a slightly better iron chelator. This small difference in the complexation behaviour of these compounds towards the two metal ions may be ascribed to some extra difficulty in disrupting the hydrogen-bonding network of $NTA(BuHP)_3$ for wrapping the metal ion with larger dimensions, such as Fe^{3+} compared with Al^{3+} (ionic radius 65 and 52 pm, respectively). Moreover, $NTA(BuHP)_3$ and $NTP(PrHP)_3$ appear to be stronger Al/Fe chelators than $Kemp(BuHP)_3$ and $Kemp(PrHP)_3$, respectively. That may be due to the higher backbone flexibility of the nitrilo- than the Kemp-based derivatives, with enhancement of the metal wrapping ability and the complex stability. Furthermore, in opposition to the Kemp derivatives,

identical arm flexibility could be expected for these compounds under study, due to the same number and type of atoms between the anchoring tertiary amine and the chelating moieties, but the different positioning of the attachment point (amide linkage) of both sub-arms contribute to some differences in complex formation.

Comparison between the metal (M) chelating affinities of ligands with different proton dependency and denticity is usually made on the basis of pM values (pM $= -\log$ [M] with $C_L/C_M = 10$ and $C_M = 10^{-6}$ M) at a specific pH, usually physiological pH (7.4). Therefore, pM values were calculated for the Fe and Al complexes with the ligands under study and are depicted on Table 2, together with the corresponding

Table 2. The pM[a] values at physiological pH for the ligands under study and other reported chelators.

Ligand	pFe	pAl
NTP(PrHP)₃	29.4	22.4
NTA(BuHP)₃	27.9[b]	22.0
Kemp(PrHP)₃[15]	28.0	21.2
Kemp(BuHP)₃[15]	26.8	21.8
Tren(Me-3,2-HOPO)[24]	26.7	–
3,4-LI(Me-3,2-HOPO)[25]	25.5	–
CP254[26]	27.2	–
IDA(3,4-HP)₂[27]	25.8	18.8
EDTA(3,4-HP)₂[12]	26.3	19.0
HBED[28]	30.9	–
EDTA[29]	23.4	16.2
DTPA[29]	24.6	15.7
DFO[30,31]	26.5	19.3
DFP[19]	19.3	16.0
transferrin[30,32]	20.3	14.5

[a] $C_M = 10^{-6}$ M, $C_L/C_M = 10$. [b] No precipitation for the low concentration values of pM determination.

values for a set of synthetic and biological ligands, namely, polyhydroxypyridinone-based ligands, such as hexadentate 3,2-HP (tripodal Tren(Me-3,2-HOPO) (Tren = tris(2-aminoethyl)amine, Me-3,2-HOPO = 1-methyl-3,2-hydroxypyridinone),[24] linear 3,4-LI(Me-3,2-HOPO) (3,4-LI = N¹-(3-aminopropyl)butane-1,4-diamine),[25] a hexadentate tripodal 3,4-HP (CP254),[26] tetradentate 3,4-HP (IDA(3,4-HP)₂ (IDA = iminodiacetic acid),[27] EDTA(3,4-HP)₂[12]), and some well known non-hydroxypyridinone strong synthetic chelators such as N,N'-bis(2-hydroxybenzyl)ethylenediamine-N,N'-diacetic acid (HBED),[28] EDTA,[29] DTPA = diethylene triamine pentaacetic acid,[29] desferrioxamine (DFO),[30,31] DFP,[19] and the endogenous ligand, transferrin.[30,32] Analysis reveals that the herein developed hexadentate chelators are more potent than the others, except HBED, reported in Table 2 towards iron. Thus, the high metal chelating affinity revealed by these novel hexadentate hydroxypyridinones undoubtedly constitutes a strong motivating factor for pursuing biodistribution studies with both ligands to evaluate their removal capacity towards hard metal ions.

Based on the known similar high chelating affinity of 3,4-HP ligands for hard metal ions (M³⁺: M = Fe, Al, Ga)[15] and on a preliminary evaluation of the capacity of one of these

hexadentate ligands towards Ga³⁺ (pGa = 27.29 for NTP-(PrHP)₃[33]), a gallium radiotracer (⁶⁷Ga) was used as in vivo model for the iron mobilisation studies (see below).

Molecular modelling of the iron complexes: Since efforts to obtain good crystalline samples of the ferric complexes for X-ray diffraction have been unsuccessful up to now (although trials are still on going), it was decided to carry out molecular modelling studies to provide further insight into both ferric complex structures. Therefore, molecular simulations were carried out with full geometry optimisation of the iron complexes by quantum mechanical calculations based on DFT methods included in the Gaussian 03 program software,[34] with the B3LYP hybrid functional.[35] No symmetry constrains were enforced during geometry optimisation. Both energy-minimised complex structures are quite similar in terms of the metal hexacoordination and octahedral geometry (Figure 5), in agreement with our expectations and solution spectroscopic parameters.
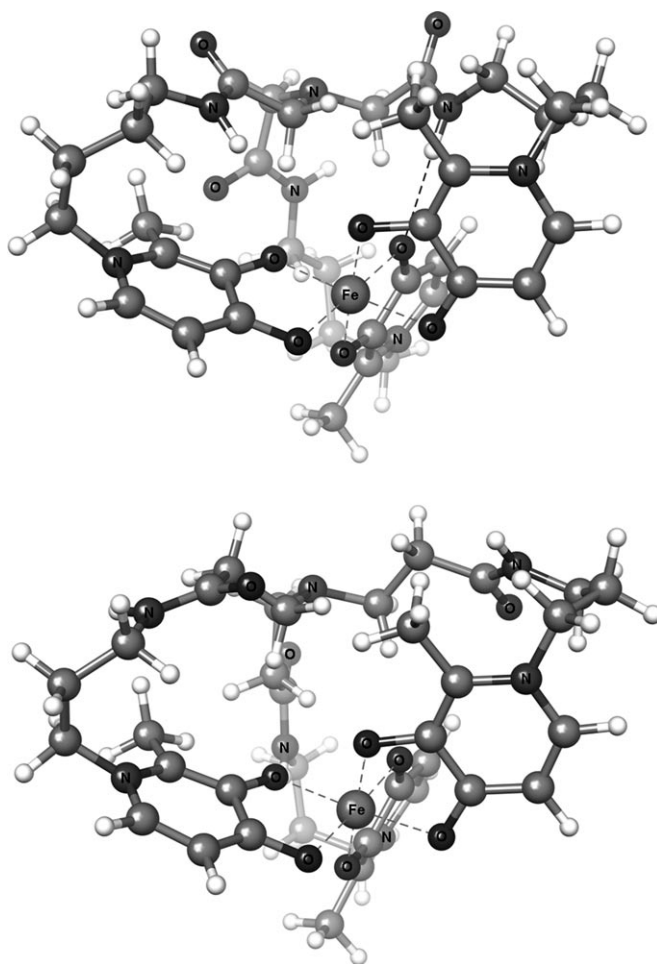

Figure 5. DFT-minimised structures of complexes Fe³⁺–L with NTA-(BuHP)₃ (top) and NTP(PrHP)₃ (bottom). Dashed lines: O−Fe metal octahedral coordination bonds (grey); hydrogen bond (black). For clarity, only heteroatoms are labelled, while carbon atoms are coloured grey and hydrogen atoms are white.

According to chemical intuition, both minimum-energy structures have an "out" conformation, which means that the tertiary amine N atom and the free electron pair is pointing away from the metal ion. However, interestingly, the "in" conformation was found in the X-ray structure of the ferric complex with a tripodal hexadentate 3-hydroxy-2-pyridinone (FeCP130).[36] Direct comparison between the studied and the reported model structures cannot be made due to differences in the anchoring skeletons (nitrilotricarboxylic acids versus trisaminoethylamine) and in the chelating units (3-hydroxy-4-pyridinone and 3-hydroxy-2-pyridinone). However, in the present case, it is believed that the "in" conformation may be favoured for the free ligand, due to an increased number of stabilising intramolecular hydrogen bonds, whereas these interactions have to be disrupted to pre-organise the ligand geometry for the metal wrapping and coordination by the chelating arms. All of the amide protons point outwards from the molecule, but in the Fe–NTA(BuHP)$_3$ complex one of them is pointing inwards and forms an intramolecular hydrogen bond with a chelating carbonyl O-atom from the neighbouring arm (hydrogen-bond length NH···O 2.23 Å; hydrogen-bond angle N-H-O 170°). This type of intramolecular hydrogen bond is quite often found in this family of complexes[37] and in the NTA derivative it can be due to the higher number of hydrogen-bond donors and acceptors in a closer distance as well as to the higher flexibility of the HP arm, relative to the NTP derivative. The oxygen atom participation in that hydrogen bond should result in a change in its electronegativity, thus justifying the lengthening of the corresponding O−Fe bond (1.999 Å), compared with the average value (1.950 Å) found in these complexes, although still in the range of values reported in the literature for the X-ray crystal structure of the ferric complex with other 3-hydroxy-4-pyridinones (DFP).[37]

Since both complexes under study have the same number and type of atoms, their stability can be compared on the basis of differences between their total energies. The calculated minimum energies are very close (but (Fe–NTP(PrHP)$_3$ is slightly more stable than Fe–NTA(BuHP)$_3$; $\Delta E = 0.004718$ hartree $= 2.960$ kcal mol^{-1}), thus suggesting analogous stabilities for both complexes. Based on the above cited calculated hydrogen-bond parameters, this hydrogen bond should have a weak to moderate strength (2–7 kcal mol^{-1}).[38,39] However, it has been determined that, in the case of weak interactions, DFT procedures may be deficient due to their inability to take into account the dispersion energy.[39] Therefore, this intramolecular hydrogen bond may not have an important contribution to the molecular stability of the NTA complex derivative, or its stabilising effect is overcome by other structural (metal ion wrapping) and electrostatic contributions that determine the overall stability of these ferric complexes. These simulations are somehow corroborated by the solution complexation studies, showing that the Fe–NTP(PrHP)$_3$ complex is only slightly more stable than Fe–NTA(BuHP)$_3$, and so the position of the amide linkage in the chelating arm does not seem to be very dependent on the stability of these complexes.

Biodistribution studies: To evaluate the efficacy of the new hexadentate ligands (NTA(BuHP)$_3$ and NTP(PrHP)$_3$) as chelating agents for mobilisation of hard metal ions, the effect of these compounds on the usual biodistribution profile of the ^{67}Ga–citrate was studied through tissue distribution biokinetics in female mice, after intravenous administration of the radiotracer. The biological distribution of this radiotracer was compared with that involving the simultaneous intraperitoneal administration of 0.5 μmol of each ligand in saline solution. The most representative tissue distribution data are shown in Figure 6. Both hexadentate li-
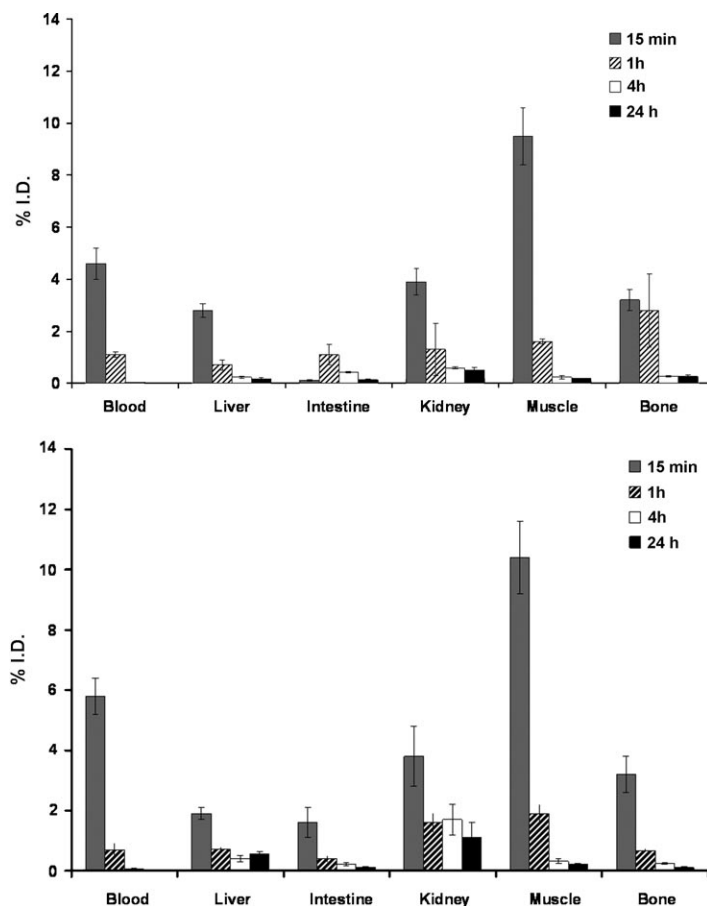

Figure 6. Biodistribution data in the most relevant organs, expressed as % I. D. per organ for ^{67}Ga–citrate with simultaneous intraperitoneal injection of the ligand NTA(BuHP)$_3$ (top) or NTP(PrHP)$_3$ (bottom) at 15 min, 1 h, 4 h and 24 h, after intravenous administration in female mice ($n = 3$–5).

gands induce similar modifications on the radiotracer biodistribution, but NTA(BuHP)$_3$ provoked slightly slower blood and bone clearance than NTP(PrHP)$_3$, as well as concomitantly slower hepatobiliar and whole animal body radioactivity excretion. However, these differences are actually very small, as expected from the similarity of the ligand properties in terms of lipophilicity and metal chelating affinity.

These results clearly show that the co-administration of any of these ligands induces a rapid clearance of the radio-tracer from most tissues, especially blood, muscle and bone, and greatly increases the overall excretion rate of radioactivity from the whole animal body. Moreover, no significant uptake in any major organ, except those related with excretory routes was found. Such improvement in the elimination of the radiotracer illustrates the clear ability of these ligands to coordinate in vivo with gallium, thus acting as removal agents for this metal. Therefore, this biodistribution pattern suggests the potential application of these ligands to complex and to eliminate in vivo overdoses of hard trivalent metal ions.

To confirm the high in vivo chelating efficiency of the ligand for the radiometal, the ^{67}Ga complexes of these ligands were prepared with high labelling efficiency and their biodistribution evaluated in the same animal model 4 h after injection (data not shown). Comparison between the biodistribution profiles of the complexes and those of the radio-tracer (^{67}Ga–citrate) followed by injection of the related ligands do not present significant differences in the uptake and clearance from the main organs as well as on the excretion rate. These observations indicate that the biodistribution of the tracer with co-administration of the ligand should correspond to the in vivo formation of the ^{67}Ga complex.

Comparison between ^{67}Ga-mobilisation ability of the new ligands (NTA(BuHP)$_3$, NTP(PrHP)$_3$) and of other 3,4-HP-based compounds (e.g., hexadentate (Kemp(PrHP)$_3$), tetradentate (IDA(PrHP)$_2$) and bidentate (DFP) ligands) can be made by analysis of the data shown in Figure 7, which illustrates the effect on biodistribution of ^{67}Ga in mice, when the radiotracer is co-administrated with the chelators.

Although each of the five ligands can modify the ^{67}Ga biological distribution pattern, enhancing its total excretion, significant differences were observed on the clearance from

major organs and especially on the excretion rate. All of the reported hexa- and tetradentate ligands[15,27] are highly efficient to eliminate radioactivity from the animal body. Nevertheless, the administration of NTA(BuHP)$_3$ or NTP(PrHP)$_3$ led to a even faster clearance from main organs than Kemp-(PrHP)$_3$ or IDA(PrHP)$_2$, which can be attributed to improved properties of the new compounds in terms of lipo-hydrophilic balance and metal affinity. Concerning the commercially available iron-chelating drug, DFP, the most significant differences (data in the histogram of Figure 7) are the fastest clearance from main organs induced by the co-administration of the hexadentate ligands (NTA(BuHP)$_3$ and NTP(PrHP)$_3$) and the overall excretion enhancement. In fact, the overall excretion induced by the new ligands is quite rapid, as indicated by the ^{67}Ga I.D values at 15 min, 1 h, 4 h and 24 h of 36.5, 77.2, 92.2 and 97.0%, respectively, in the presence of NTP(PrHP)$_3$ and 39.0, 72.4, 95.3 and 96.0%, respectively, in the presence of NTA(BuHP)$_3$.

In summary, the favourable biodistribution and excretion profiles associated with the administration of these new chelators, especially the biological profile of the radiotracer with co-administration of the hexadentate ligands, indicates the in vivo formation of a complex with fast tissue clearance and rapid excretion. These are essential requirements to get a high ratio between target/not target organs and highlight the interest to synthesise new radioactive complexes with ligands containing a similar backbone for specific targeting.

Conclusion

Two novel tripodal hexadentate 3,4-HP-based chelators have been designed, prepared and then studied in solution and in vivo for their properties as potential iron or aluminium sequestering agents for metal chelating therapy.

Both compounds have aminotricarboxylic anchoring backbones attached to aminoalkyl bidentate 3,4-HP chelating moieties, but differing in the positioning of the peptidic bonds connecting the tripodal carboxylate (NTA or NTP) and HP-chelating segments. Although both isomeric ligands have the same arm size, considerable differences result from the hydrogen-bonding networks associated with the apical amine, namely, the five- and six-membered ring hydrogen-bonded intermediates associated with the NTA and NTP derivatives, respectively. These differences were mostly reflected in the acidity of the corresponding ammonium protons. Both compounds revealed higher chelating capacity than other reported hydroxypyridinone-based ligands, although NTP(PrHP)$_3$ is a slightly stronger chelator than NTA-(BuHP)$_3$, in agreement with the analogous results found for the calculated minimum-energy structures of the iron complexes and respective total energies. Concerning the in vivo metal mobilisation, both evidenced excellent capacities, especially in comparison with other reported polydentate 3,4-HP chelators. Furthermore, the favourable biodistribution profiles and high excretion rates, resulting from the administration of NTA(BuHP)$_3$ or NTP(PrHP)$_3$, support expecta-
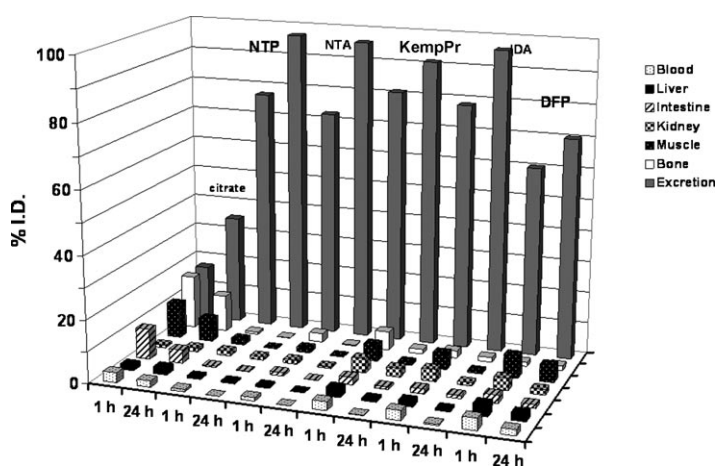

Figure 7. Biodistribution data in the most relevant organs, expressed as % I. D. per organ for ^{67}Ga–citrate and ^{67}Ga–citrate with simultaneous intraperitoneal injection of the ligands NTP(PrHP)$_3$, NTA(BuHP)$_3$, Kemp-(PrHP)$_3$, IDA(PrHP)$_2$ or DFP, 1 and 24 h after intravenous administration in female mice ($n=3$–5).

tions on the potential clinical application of these novel ligands as useful metal removal agents.

Experimental Section

General remarks: All the chemicals were of analytical reagent grade and used as supplied without further purification. Whenever necessary, the organic solvents were dried according to standard methods.[40] In the complexation studies, the solutions of FeCl$_3$ (0.0177 M) and AlCl$_3$ (0.0393 M) from Merck were standardised by atomic absorption. These solutions were prepared in excess acid to prevent hydrolysis and their exact concentration in HCl was determined by titration with HCl 0.1 M (Titrisol) for values of pH $\geq$ 2.

^{1}H NMR spectra were recorded on a Varian Unity 300 MHz or a Bruker Advance II 300 spectrometer. Chemical shifts are reported in ppm (δ) from internal references TMS (tetramethylsilane) for organic solvents and DSS ([D$_4$]3-trimethylsilylpropionic acid sodium salt) for D$_2$O. The titrant (0.1 M KOH) was prepared from a carbonate-free commercial concentrate (Titrisol) and standardised by titration with a solution of potassium hydrogen phthalate. It was discarded whenever the percentage of carbonate (Gran's method)[41] was higher than 0.5% of the total amount of base.

Elemental analyses were performed on a Fisons EA1108 CHNF/O instrument. Electronic spectra were recorded with a Perkin–Elmer Lambda 9 spectrophotometer, using 1 cm path length cells that were thermostated at (25.0 ± 0.1)°C by a Grant W6 equipment.

1-(4-Aminobutyl)-3-benzyloxy-2-methylpyridin-4(1H)-one (1): A solution of 2 M NaOH (2 mL) was added to a solution of 1,4-diaminobutane (3 mL, 30 mmol) in 1:1 ethanol/water (50 mL) and heated to 50°C; then a solution of 3-benzyloxy-2-methyl-4-pyrone, prepared as previously described[27] (6.0 g, 28 mmol) in ethanol (25 mL), was added dropwise, and the mixture was stirred overnight at 60°C. The solvent was removed and the residue was dried under vacuum. The crude product was dissolved in water (30 mL), the solution was acidified to pH 1 with concentrated HCl, and then it was washed with dichloromethane (3×30 mL); afterwards the aqueous solution was neutralised with 5% NaOH and then further extracted with dichloromethane (3×30 mL). The aqueous phase was basified to pH 12 (with 5% NaOH) and then was extracted with dichloromethane (5×30 mL). The organic phases were dried over anhydrous Na$_2$SO$_4$ and the solvent was removed under vacuum. An HCl-saturated methanolic solution was added to acidify the residue until obtaining pH 1 and the solvent was then removed. The pure dihydrochloric salt of **1** was obtained after recrystallisation from dry methanol/acetonitrile, as a yellowish solid (4.1 g, 48%). M.p. 115–117°C; ^{1}H NMR (D$_2$O): δ = 7.75 (d, J = 7.2 Hz, 1H; 6-PyH), 7.41 (s, 5H; PhH), 6.61 (d, J = 7.2 Hz, 1H; 5-PyH), 5.05 (s, 2H; CH_2Ph), 4.03 (t, J = 7.4 Hz, 2H; CH_2Py), 2.98 (t, J = 7.5 Hz, 2H; NH$_2$CH_2(CH$_2$)$_3$Py), 2.10 (s, 3H; CH_3), 1.71 (q, J = 7.2 Hz, 2H; (CH$_2$)$_2$CH_2CH$_2$Py), 1.62 ppm (q, J = 6.8 Hz, 2H; CH$_2$CH_2(CH$_2$)$_2$Py); m/z (FAB): 287 [M+H]$^+$.

2,2′,2″-Nitrilotris(N-{4-[3-benzyloxy-2-methyl-4-oxopyridin-1(4H)-yl]butyl}acetamide) (2): TBTU (1.1 mL, 3.3 mmol) and dry NMM (0.70 mL, 6.3 mmol) were added to a solution of NTA (0.19 g, 1.0 mmol) in dry DMF (10 mL) at 0°C and the reaction mixture was stirred for 45 min under N$_2$. Meanwhile, compound **1** (1.11 g, 3.1 mmol) in dry DMF (15 mL) was neutralised with NMM (0.68 mL, 6.2 mmol) and mixture was stirred at RT for 30 min; the first solution was added dropwise to the free amine and it was left stirring overnight. After evaporation of the reaction-mixture solvent, the residue was dissolved in dichloromethane (50 mL) and extractions were performed with 5% aqueous NaOH (2×20 mL) and brine (2×20 mL); the final organic phase was dried over anhydrous Na$_2$SO$_4$ and evaporated. Flash chromatography was performed on silica gel, using 2:0.6:0.01 acetonitrile/water/concd ammonia as the eluent (R_f = 0.32). After evaporation of the solvent, dry acetonitrile was added to the residue and the insoluble inorganic matter was filtered off. Evaporation of the solvent afforded the pure product as a pale yellow solid (0.61 g, 61%). M.p. 90–91°C; ^{1}H NMR (D$_2$O, pD, ca. 3): δ = 7.82 (d,

J = 7.2 Hz, 3H; 6-PyH), 7.36 (m, 15H; PhH), 6.75 (d, J = 7.2 Hz, 3H; 5-PyH), 5.02 (s, 6H; CH_2Ph), 4.01 (t, J = 7.2 Hz, 6H; CH_2Py), 3.34 (s, 6H; NCH_2CONH), 3.14 (t, J = 6.6 Hz, 6H; CONHCH_2(CH$_2$)$_3$Py), 2.10 (s, 9H; CH_3), 1.58 (q, J = 7.5 Hz, 6H; CONH(CH$_2$)$_2$CH_2CH$_2$Py), 1.40 ppm (q, J = 7.4 Hz, 6H; CONHCH$_2$CH_2(CH$_2$)$_2$Py); m/z (FAB): 997 [M+H]$^+$.

2,2′,2″-Nitrilotris(N-{4-[3-hydroxy-2-methyl-4-oxopyridin-1(4H)-yl]butyl}acetamide) (NTA(BuHP)$_3$): 10% Pd/C (0.090 g) was added to a solution of **2** (0.18 g, 0.18 mmol) in methanol (10 mL) and the mixture was stirred under H$_2$ (1.5 bar) for 3 h. After filtration and removal of the solvent, recrystallisation from dry methanol/ethyl ether afforded the pure compound as a pale yellow solid (0.12 g, 89%). M.p. 159–160°C; ^{1}H NMR (D$_2$O): δ = 7.94 (d, J = 7.2 Hz, 3H; 6-PyH), 7.00 (d, J = 6.9 Hz, 3H; 5-PyH), 4.23 (t, J = 7.6 Hz, 6H; CH_2Py), 4.04 (s, 6H; NCH_2CONH), 3.17 (t, J = 6.9 Hz, 6H; CONHCH_2(CH$_2$)$_3$Py), 2.45 (s, 9H; CH_3), 1.72 (q, J = 7.2 Hz, 6H; CONH(CH$_2$)$_2$CH_2CH$_2$Py), 1.48 ppm (q, J = 7.3 Hz, 6H; CONHCH$_2$CH_2(CH$_2$)$_2$Py); m/z (FAB): 726 [M+H]$^+$; elemental analysis calcd (%) for C$_{36}$H$_{51}$N$_7$O$_9$·0.8 MeOH: C 58.82, H 7.27, N 13.05; found: C 58.90, H 7.01, N 12.81.

3,3′,3″-Nitrilotris(N-{3-[3-benzyloxy-2-methyl-4-oxopyridin-1(4H)-yl]propyl}propanamide) (3): A procedure similar to that used for the preparation of **2** was followed, starting from NTP and 1-(3′-aminopropyl)-3-benzyloxy-2-methylpyridin-4(1H)-one dihydrochloride.[27] After performing the extractions and evaporating the organic solvent, flash chromatography was performed on silica gel using 2:1:0.02 acetonitrile/water/concd ammonia as the eluent (R_f = 0.27). After evaporation of the solvent, the inorganic matter was removed by the addition of (2:1) dry acetonitrile/methanol and filtration of the mixture. Evaporation of the solvent afforded the pure product as a pale hygroscopic solid (0.39 g, 39%). ^{1}H NMR (D$_2$O, pD ca. 3): δ = 8.14 (d, J = 7.1 Hz, 3H; 6-PyH), 7.37 (s, 15H; PhH), 7.15 (d, J = 7.1 Hz, 3H; 5-PyH), 5.07 (s, 6H; CH_2Ph), 4.22 (t, J = 7.5 Hz, 6H; CH_2Py), 3.45 (t, J = 5.8 Hz, 6H; NCH_2CH$_2$CONH), 3.12 (t, J = 6.7 Hz, 6H; CONHCH_2CH$_2$CH$_2$Py), 2.83 (t, J = 5.7 Hz, 6H; NCH$_2$CH_2CONH), 2.30 (s, 9H; CH_3), 1.88 ppm (q, J = 7.4 Hz, 6H; CONHCH$_2$CH_2CH$_2$Py); m/z (FAB): 997 [M+H]$^+$.

3,3′,3″-Nitrilotris(N-{3-[3-hydroxy-2-methyl-4-oxopyridin-1(4H)-yl]propyl}propanamide) (NTP(PrHP)$_3$): Catalytic hydrogenation of **3** was performed as described for NTA(BuHP)$_3$. In this case, the reaction mixture was filtered and the solvent was removed under vacuum, then the residue was washed with a dichloromethane/acetonitrile mixture. Final recrystallisation from dry methanol/ethyl ether afforded the pure product as a pale hygroscopic solid (0.14 g, 88%). ^{1}H NMR (D$_2$O, pD ca. 3): δ = 8.02 (d, J = 7.2 Hz, 3H; 6-PyH), 7.08 (d, J = 6.9 Hz, 3H; 5-PyH), 4.34 (t, J = 7.5 Hz, 6H; CH_2Py), 3.47 (t, J = 5.8 Hz, 6H; NCH_2CH$_2$CONH), 3.23 (t, J = 6.6 Hz, 6H; CONHCH_2CH$_2$CH$_2$Py), 2.86 (t, J = 5.7 Hz, 6H; NCH$_2$CH_2CONH), 2.54 (s, 9H; CH_3), 2.01 ppm (q, J = 7.3 Hz, 6H; CONHCH$_2$CH_2CH$_2$Py); m/z (FAB): 726 [M+H]$^+$; elemental analysis calcd (%.) for C$_{36}$H$_{51}$N$_7$O$_9$: C 59.57, H 7.08, N 13.51; found: C 59.65, H 7.42, N 13.48.

Potentiometric titrations

Measurements: Potentiometric titrations of the ligands and their aluminium complexes were performed in water at ionic strength (I) 0.1 M KCl, T = (25.0 ± 0.1)°C and the equipment used was previously described.[42] For the system Fe^{3+}–NTA(BuHP)$_3$ study, the calibration procedure was analogous to that in aqueous medium, but in a water/DMSO (97:3) solvent mixture. For all of the samples prepared, the total volume was 20 mL, the ligand concentration (C_L) was 1.0–1.7×10^{-3} M and the metal ion to ligand molar ratio was 0:1 or 1:1. Each titration was performed twice and the value determined for the ionisation constant (pK_w) was 13.85 and 13.80 for the water and 3% DMSO media, respectively.

Calculation of equilibrium constants: The stepwise protonation constants, K_i = [H$_i$L]/[H$_{i-1}$L][H], (excluding the logK_D value for NTA(BuHP)$_3$) and the overall aluminium complex stability constants, $\beta_{M_mH_hL_l}$ = [Al$_m$H$_h$L$_l$]/[Al]^m[H]^h[L]^l, were calculated by the fitting analysis of the respective potentiometric data with the HYPERQUAD 2003 program.[23] The Al^{3+} hydrolytic species[43] were included in the equilibrium model and the species distribution curves were plotted with the HYSS program.[23]

Spectroscopic titrations

Measurements: ^{1}H NMR titration of a solution of NTA(BuHP)$_3$ (7.3×10^{-4} M) in D$_2$O was performed as previously described.[42, 44]

The electronic spectra of the Fe^{III} complexes with both ligands were recorded in the range 300–750 nm and 1:1 stoichiometry ($C_L = 1.8 \times 10^{-4}$ M for NTA(BuHP)$_3$ and 1.6×10^{-4} M for NTP(PrHP)$_3$). Solutions of complexes with pH ≥ 2 were prepared as indicated for the potentiometric measurements. Both Fe^{3+}–L systems were studied for pH below 2 (0.6–2, for L=NTA(BuHP)$_3$); 0.8–2 for L=NTP(PrHP)$_3$) using a batch titration (7–13 points), in which the amount of acid to be added (from standard 0.1 or 1 M HCl solutions) was calculated for the total volume solution used. To improve the low water solubility of the FeL complex of NTA-(BuHP)$_3$, the iron complexation of that ligand was studied in a 3% (v/v) DMSO/water medium.

Calculation of equilibrium constants: The logK_D value was calculated by fitting analysis of the experimental data, using the PSEQUAD program[22] and then that value (determined in D$_2$O) was converted into the corresponding value in H$_2$O by the equation p$K_D = 0.32 + 1.044$pK_H.[45] The overall iron complex stability constants were determined with the PSEQUAD program,[22] by fitting of the spectrophotometric data and including the Fe^{3+} hydrolytic species[43] in the equilibrium model.

Partition coefficients: The octanol–water partition coefficients (log$P$) were determined by the "shakeflask" method,[8, 46] based on the concentration ratio of the compound between 1-octanol and a Tris-buffered aqueous phase (pH 7.4). The species concentrations were evaluated by spectrophotometry, based on the absorbance of the benzenoid bands (π–π*) of the compounds.

ESI-MS measurements: The electrospray mass spectra were obtained on ESI-QIT/MS Bruker HCT (electrospray ionisation quadrupole ion trap mass spectrometer), operated in the positive mode. The temperature of the heated capillary was set at 250 °C. The flow rate of the electrospray solution was 2.5 μL min^{-1}. Other parameters, including capillary, capillary exit, skimmer voltage (4 kV, 150 V, 40 V), nebuliser/N$_2$ pressure 8.0 psi. Solutions of metal and ligand ($C_M/C_L = 1$, $C_L = 1 \times 10^{-4}$ M) in water were analysed at appropriate pH values: 2.96 (Fe^{3+}–NTA(BuHP)$_3$), 3.83 (Al^{3+}–NTA(BuHP)$_3$), 3.50 (Fe^{3+}–NTP(PrHP)$_3$) and 3.96 (Al^{3+}–NTP(PrHP)$_3$).

Molecular modelling: The structure of Fe^{3+}–L complexes with NTA-(BuHP)$_3$ and NTP(PrHP)$_3$ were fully optimised by quantum mechanical calculations based on DFT methods included in the Gaussian 03W program software.[34] A first optimisation step was carried out using the B3LYP chemical model with a LANL2MB basis set, a direct SCF calculation and an SCF convergence criterion to 10^{-5}. The B3LYP chemical model has been shown to be an accurate density functional method,[47] and it gives as good or better geometries and energies as MP2 ab initio methods for first-row transition-metal complexes.[48] The B3LYP model is a combination of the Becke three-parameter hybrid functional[35] with the Lee–Yang–Parr correlation functional (which also includes density gradient terms).[49, 50] With regards to the basis set, LANL2MB specifies the STO-3G on first row[51] and, Los Alamos ECP plus MBS on Na-Bi.[52] The results of these calculations were then subjected to a deeper optimisation using the B3LYP model with the LANL2DZ basis set that describes the Fe atom through the Los Alamos ECP and an essentially double-zeta basis set including 3d orbitals and 3d diffuse functions for the valence shell. In this basis set, the rest of the atoms are described through the Dunning–Huzinaga full double-ζ basis set.[53]

Biodistribution studies: A ^{67}Ga–citrate injection solution was prepared by dilution of ^{67}Ga–citrate purchased from MDS Nordion (Ottawa, Canada) with saline to obtain a final radioactive concentration of 5–10 MBq/100 μL. Animal studies were carried out in groups of 3–5 female CD1 mice (randomly bred, Charles River, from CRIFFA, Barcelona, Spain) weighing around 25 g. Mice were intravenously (i.v.) injected with ^{67}Ga–citrate (100 μL, 5–10 MBq) through the tail vein. In a separate group of animals, the i.v. administration was immediately followed by intraperitoneal (i.p.) injection of the ligand (0.5 μmol) in saline solution (100 μL). Animals were maintained on a normal diet ad libitum and were sacrificed by cervical dislocation at 5 min, 30 min, 1 h and 24 h post-administration. The administered radioactive dose and the radioactivity in sacrificed animals were determined by counting in a dose calibrator

(Aloka, Curiemeter IGC-3, Aloka, Tokyo, Japan). The difference between the radioactivity in the injected and sacrificed animal was assumed to be due to whole body excretion. Tissue samples of main organs were then removed for counting in a gamma counter (Berthold LB2111, Berthold Technologies, Germany). Biodistribution results were expressed as percent of injected dose per total organ (%ID/organ) and presented as mean values ±standard deviation. For blood, bone and muscle, total activity was calculated by assuming, as previously reported, that these organs constitute 7, 10 and 40% of the total weight, respectively.

Animal experiments were carried out by a researcher holding certification by the National Authority in accordance with the EU recommendations on the use of living animal in scientific investigation and followed the principles of laboratory animal care.

[1] R. R. Crichton, *Inorganic Biochemistry of Iron Metabolism: From Molecular Mechanisms to Clinical Consequences*, Wiley, New York, **2001**.

[2] T. Kiss, K. Gajda-Schrantz, P. Zatta, *Neurodegenerative Diseases and Metal Ions*, Wiley, New York, **2006**.

[3] M. K. Ward, T. G. Feest, H. E. Ellis, I. S. Parkinson, D. N. S. Kerr, J. Herrington, G. L. Goode, *Lancet* **1978**, *311*, 841–845.

[4] G. Crisponi, M. Remelli, *Coord. Chem. Rev.* **2008**, *252*, 1225–1240.

[5] M. A. Santos, *Coord. Chem. Rev.* **2002**, *228*, 187–203.

[6] G. J. Kontoghiorghes, *Lancet* **1985**, *325*, 817–817.

[7] a) M. Y. Moridani, G. S. Tilbrook, H. H. Khodr, R. C. Hider, *J. Pharm. Pharmacol.* **2002**, *54*, 349–364; b) R. C. Hider, Z. D. Liu, *Curr. Med. Chem.* **2003**, *10*, 1051–1064.

[8] M. A. Santos, M. Gil, L. Gano, S. Chaves, *J. Biol. Inorg. Chem.* **2005**, *10*, 564–580.

[9] D. E. Green, C. L. Ferreira, R. V. Stick, B. O. Patrick, M. J. Adam, C. Orvig, *Bioconjugate Chem.* **2005**, *16*, 1597–1609.

[10] K. H. Thompson, C. A. Barta, C. Orvig, *Chem. Soc. Rev.* **2006**, *35*, 545–556.

[11] E. Nisbet-Brown, N. F. Olivieri, P. J. Giardina, R. W. Grady, E. J. Neufeld, R. Sechaud, A. J. Krebs-Brown, J. R. Anderson, D. Alberti, K. C. Sizer, D. G. Nathan, *Lancet* **2003**, *361*, 1597–1602.

[12] S. Gama, E. Farkas, P. I. Dron, S. Chaves, M. A. Santos, *Dalton Trans.* **2009**, 6141–6150.

[13] a) M. A. Santos, *Coord. Chem. Rev.* **2008**, *252*, 1213–1224; b) S. Chaves, P. I. Dron, F. A. Danalache, D. Sacoto, L. Gano, M. A. Santos, *J. Inorg. Biochem.* **2009**, *103*, 1521–1529.

[14] S. Piyamongkol, T. Zhou, Z. D. Liu, H. Khodr, R. C. Hider, *Tetrahedron Lett.* **2005**, *46*, 1333–1336.

[15] R. Grazina, L. Gano, J. Sebestik, M. A. Santos, *J. Inorg. Biochem.* **2009**, *103*, 262–273.

[16] M. A. Santos, R. Grazina, L. Gano, S. Gama, Port. Pat. PT102660, **2003**.

[17] E. T. Clarke, A. E. Martell, *Inorg. Chim. Acta* **1992**, *196*, 185–194.

[18] R. A. Yokel, A. K. Datta, E. G. Jackson, *J. Pharmacol. Exp. Ther.* **1991**, *257*, 100–106.

[19] M. A. Santos, M. Gil, S. Marques, L. Gano, G. Cantinho, S. Chaves, *J. Inorg. Biochem.* **2002**, *92*, 43–54.

[20] R. M. Smith, A. E. Martell, *Critical Stability Constants, Vol 5*, Plenum, New York, **1982**, p. 62.

[21] C. A. Lipinski, F. Lombardo, B. W. Dominy, P. J. Feeney, *Adv. Drug Delivery Rev.* **1997**, *23*, 3–25.

[22] PSEQUAD version 5.01, L. Zékány, I. Nagypál, G. Peintler, **2001**.

[23] P. Gans, A. Sabatini, A. Vacca, *Talanta* **1996**, *43*, 1739–1753.

[24] I. Turcot, A. Stintzi, J. D. Xu, K. N. Raymond, *J. Biol. Inorg. Chem.* **2000**, *5*, 634–641.

[25] R. J. Abergel, K. N. Raymond, *Inorg. Chem.* **2006**, *45*, 3622–3631.

[26] T. Zhou, X. L. Kong, Z. D. Liu, D. Y. Liu, R. C. Hider, *Biomacromolecules* **2008**, *9*, 1372–1375.

[27] M. A. Santos, S. Gama, L. Gano, G. Cantinho, E. Farkas, *Dalton Trans.* **2004**, 3772–3781.

[28] A. E. Martell, R. M. Smith, *Critical Stability Constants, Vol. 1*, Plenum, New York, **1974**, p. 112; A. E. Martell, R. M. Smith, *Critical Stability Constants, Vol. 6*, Plenum, New York, **1989**, p. 55.

[29] A. E. Martell, R. M. Smith, R. J. Motekaitis, *Critically Selected Stability Constants of Metal Complexes Database*, Plenum, New York, **1997**.

[30] R. J. Motekaitis, A. E. Martell, *Inorg. Chim. Acta* **1991**, *183*, 71–80.

[31] Z. D. Liu, R. C. Hider, *Coord. Chem. Rev.* **2002**, *232*, 151–171.

[32] W. R. Harris, J. Sheldon, *Inorg. Chem.* **1990**, *29*, 119–124.

[33] A. C. Mendonça, S. Chaves, S. Marques, M. I. M. Prata, A. C. Santos, C. F. G. C. Geraldes, M. A. Santos, *J. Inorg. Biochem.* in press.

[34] Gaussian 03, Revision C.02, M. J. Frisch, G. W. Trucks, H. B. Schlegel, G. E. Scuseria, M. A. Robb, J. R. Cheeseman, J. A. Montgomery, Jr., T. Vreven, K. N. Kudin, J. C. Burant, J. M. Millam, S. S. Iyengar, J. Tomasi, V. Barone, B. Mennucci, M. Cossi, G. Scalmani, N. Rega, G. A. Petersson, H. Nakatsuji, M. Hada, M. Ehara, K. Toyota, R. Fukuda, J. Hasegawa, M. Ishida, T. Nakajima, Y. Honda, O. Kitao, H. Nakai, M. Klene, X. Li, J. E. Knox, H. P. Hratchian, J. B. Cross, V. Bakken, C. Adamo, J Jaramillo, R. Gomperts, R. E. Stratmann, O. Yazyev, A. J. Austin, R. Cammi, C. Pomelli, J. W. Ochterski, P. Y. Ayala, K. Morokuma, G. A. Voth, P. Salvador, J. J. Dannenberg, V. G. Zakrzewski, S. Dapprich, A. D. Daniels, M. C. Strain, O. Farkas, D. K. Malick, A. D. Rabuck, K. Raghavachari, J. B. Foresman, J. V. Ortiz, Q. Cui, A. G. Baboul, S. Clifford, J. Cioslowski, B. B. Stefanov, G. Liu, A. Liashenko, P. Piskorz, I. Komaromi, R. L Martin, D. J. Fox, T. Keith, M. A. Al-Laham, C. Y. Peng, A. Nanayakkara, M. Challacombe, P. M. W. Gill, B. Johnson, W. Chen, M. W. Wong, C. Gonzalez, J. A. Pople, Gaussian, Inc., Wallingford CT, **2004**.

[35] A. Becke, *Phys. Rev. A* **1988**, *38*, 3098–3100.

[36] G. Xiao, D. Helm, R. C. Hider, P. S. Dobbin, *Inorg. Chem.* **1995**, *34*, 1268–1270.

[37] J. Charalambous, A. Dodd, M. McPartlin, S. O. C. Matondo, N. D. Pathirana, H. R. Powell, *Polyhedron* **1988**, *7*, 2235–2237.

[38] J. Hermans, H. J. C. Berendsen, W. F. van Gunsteren, J. P. M. Postma, *Biopolymers* **1984**, *23*, 1513–1518.

[39] H. Szatyłowicz, *J. Phys. Org. Chem.* **2008**, *21*, 897–914.

[40] *Purification of Laboratory Chemicals*, 4th ed. (Eds:. W. L. F. Armarego, D. D. Perrin), Butterworth-Heinemann, Oxford, **1999**.

[41] F. J. C. Rossotti, H. Rossotti, *J. Chem. Educ.* **1965**, *42*, 375–378.

[42] S. Chaves, M. Gil, S. Marques, L. Gano, M. A. Santos, *J. Inorg. Biochem.* **2003**, *97*, 161–172.

[43] a) *The Hydrolysis of Cations* (Eds.: C. F. Baes, R. E. Mesmer), Wiley, New York, **1976**; b) L. O. Öhman, W. Forschling, *Acta Chem. Scand. Ser. A* **1981**, *35*, 795–802.

[44] A. K. Covington, M. Paabo, R. A. Robinson, R. G. Bates, *Anal. Chem.* **1968**, *40*, 700–706.

[45] R. Delgado, J. J. R. Fraústo da Silva, M. T. S. Amorim, M. F. Cabral, S. Chaves, J. Costa, *Anal. Chim. Acta* **1991**, *245*, 271–282.

[46] A. Leo, C. Hansch, D. Elkins, *Chem. Rev.* **1971**, *71*, 525–616.

[47] C. W. Bauschlicher, *Chem. Phys. Lett.* **1995**, *246*, 40–44.

[48] A. Ricca, C. W. Bauschlicher, *Theor. Chim. Acta* **1995**, *92*, 123–131.

[49] C. Lee, W. Yang, R. G. Parr, *Phys. Rev. B* **1988**, *37*, 785–789.

[50] B. Miehlich, A. Savin, H. Stoll, H. Preuss, *Chem. Phys. Lett.* **1989**, *157*, 200–206.

[51] J. B. Collins, P. v. R. Schleyer, J. S. Binkley, J. A. Pople, *J. Chem. Phys.* **1976**, *64*, 5142–5151.

[52] P. J. Hay, W. R. Wadt, *J. Chem. Phys.* **1985**, *82*, 299–310.

[53] T. H. Dunning, Jr., P. J. Hay in *Modern Theoretical Chemistry, Vol. 3* (Ed.: H. F. Schaefer III), Plenum, New York **1976**, pp. 1–28.